FIFTH AUSTRALASIAN CONFERENCE

on

HYDRAULICS AND FLUID MECHANICS

at

University of Canterbury, Christchurch, New Zealand

1974 December 9 to December 13

FLOWS IN DUCTS BY BOUNDARY-LAYER THEORY

by

Tuncer Cebeci* and Herbert B. Keller**

SUMMARY

In this paper we present a general method for solving the boundary-layer equations for duct flows. The method which is applicable to both laminar and turbulent flows employs the eddy viscosity concept to model the Reynolds shear stress and employs a very efficient two-point finite-difference method to solve the governing equations. In the calculations the pressure drop is treated as an eigenvalue which is approximated by a Newton iteration scheme based on satisfying a relation obtained from the conservation of mass.

Numerical results are presented for laminar and turbulent flows in the entrance region of a pipe. Comparison of calculated results show good agreement with experiment.

*Adjunct professor, Mechanical Engineering Dept., California State University at Long Beach, Long Beach, California.

**Professor of Applied Mathematics, Firestone Laboratories, California Institute of Technology, Pasadena, California.

Nomenclature

f, F	stream function
L	reference length taken equal to channel width or pipe radius
p	pressure
r	radial distance from axis of revolution, $= r_o - y$
r_o	body radius
R_L	Reynolds number, $= u_o L/\nu$
t	transverse curvature parameter $= y/L$
u, v	x- and y-components of velocity, respectively
u_c	centerline velocity
u_o	reference velocity
x	distance along body surface
y	distance normal to x
y_c	centerline distance
ε	eddy viscosity
η	transformed y-coordinate
ν	kinematic viscosity
ρ	density

Basic Equations

The boundary-layer equations for two-dimensional and axisymmetric laminar and turbulent flows are:

Continuity

$$\frac{\partial}{\partial x}(r^k u) + \frac{\partial}{\partial y}(r^k v) = 0 \tag{1}$$

Momentum

$$u\frac{\partial u}{\partial x} + v\frac{\partial u}{\partial y} = -\frac{1}{\rho}\frac{dp}{dx} + \frac{\nu}{r^k}\frac{\partial}{\partial y}\left[r^k(1 + \varepsilon/\nu)\frac{\partial u}{\partial y}\right] \tag{2}$$

Here we have used the eddy-viscosity concept to model the Reynolds shear stress term that appears in the momentum equation for turbulent flow, that is,

$$-\rho\overline{u'v'} = \rho\varepsilon\frac{\partial u}{\partial y} \tag{3}$$

In (1) and (2), k is a flow index; it is zero for two-dimensional flows and is unity for axisymmetric flows. The relation between r and r_o for a pipe is

$$r = r_o - y$$

As in external boundary layers, (1) and (2) for duct flows can be solved (with a suitable formula for ε) when they are expressed in physical coordinates or in transformed coordinates. Each coordinate system has its own advantages. In the present study we use both coordinates. At first we employ a transformation, called Falkner transformation, to express (1) and (2) in transformed coordinates $(\bar{x}, \eta)$. This transformation, like all similarity transformations, removes the singularity at $x = 0$ and stretches the y-coordinate. The latter is a very useful advantage since at first, close to the entrance region, the boundary-layer thickness is very small. The transformed variables keep the boundary-layer growth nearly constant for laminar flows. However, as the boundary-layer thickness increases with increasing x, the solutions of the governing equations in transformed coordinates lose their advantages over the physical coordinates. For this reason, when the boundary-layer-thickness reaches, say, 75-percent of the half width of the channel or radius of the pipe, it is convenient to switch to physical coordinates and seek the solution of the governing equations in new variables.

Before we discuss the procedure used in our study, we shall first express the boundary-layer equations in dimensionless quantities and put them in a more suitable form by using the Mangler transformation and then combine the continuity and the momentum equations with the use of a stream function.

The introduction of the following dimensionless quantities

$$p^* = \frac{p}{\rho u_o^2}, \quad u^* = \frac{u}{u_o}, \quad v^* = \frac{v}{u_o}\sqrt{R_L}, \quad y^* = \frac{y}{L}\sqrt{R_L}, \quad x^* = \frac{x}{L}, \quad r^* = \frac{r}{L}, \tag{4}$$

$$R_L = \frac{u_o L}{\nu}, \qquad \varepsilon^+ = \frac{\varepsilon}{\nu}$$

allows (1) and (2) to be written as

$$\frac{\partial}{\partial x^*}(r^* u^*) + \frac{\partial}{\partial y}(r^* v^*) = 0, \tag{5}$$

$$u^* \frac{\partial u^*}{\partial x^*} + v^* \frac{\partial u^*}{\partial y^*} = -\frac{dp^*}{dx^*} + \frac{1}{r^*}\frac{\partial}{\partial y^*}\left[r^*(1+\varepsilon^+)\frac{\partial u^*}{\partial y^*}\right]. \tag{6}$$

Here we have dropped the superscript k for convenience. We now introduce the Mangler transformation,

$$d\bar{x} = (r_o^k)^2 dx^* \tag{7}$$

$$d\bar{y} = r^* dy^* \tag{8}$$

to place (5) and (6) into a form nearly two-dimensional, that is,

$$\frac{\partial \bar{u}}{\partial \bar{x}} + \frac{\partial \bar{v}}{\partial \bar{y}} = 0 \tag{9}$$

$$\bar{u}\frac{\partial \bar{u}}{\partial \bar{x}} + \bar{v}\frac{\partial \bar{u}}{\partial \bar{y}} = -\frac{dp^*}{d\bar{x}} + \frac{\partial}{\partial \bar{y}}\left[(1-t)^2(1+\varepsilon^+)\frac{\partial \bar{u}}{\partial \bar{y}}\right]. \tag{10}$$

Here $\bar{u}$ and $\bar{v}$ are related to u^* and v^* through

$$u^* = \bar{u}, \qquad v^* = \frac{(r_o^*)^2}{r^*}\bar{v} - \frac{\bar{u}}{r^*}\frac{\partial \bar{y}}{\partial x^*} \tag{11}$$

and t, known as the transverse curvature parameter, is defined by

$$t = 1 - \frac{r^*}{r_o^*} = \frac{y^*}{r^*\sqrt{R_L}} = 1 - \left(1 - \frac{2\bar{y}}{\sqrt{R_L}}\right)^{1/2} \tag{12}$$

With the introduction of stream function defined by

$$\bar{u} = \frac{\partial F}{\partial \bar{y}}, \qquad \bar{v} = -\frac{\partial F}{\partial \bar{x}} \tag{13}$$

we can write (10) as

$$(bF'')' = \frac{dp^*}{d\bar{x}} + F'\frac{\partial F'}{\partial \bar{x}} - F''\frac{\partial F}{\partial \bar{x}} \tag{14}$$

Here primes denote differentiation with respect to $\bar{y}$, and b is defined by

$$b = (1 - t)^2(1 + \varepsilon^+) \tag{15}$$

We define the Falkner transformation by

$$\xi = \bar{x} \tag{16}$$

$$\eta = \frac{\bar{y}}{\sqrt{\xi}},$$

and introduce another stream function $f(\xi,\eta)$ related to $F(\bar{x},\bar{y})$ by

$$F(x,y) = \sqrt{\xi}\, f(\xi,\eta) . \tag{18}$$

With this transformation, we can write (14) as

$$(bf'')' + \frac{1}{2} ff'' = \xi \frac{dp^*}{d\xi} + \xi\left(f' \frac{\partial f'}{\partial \xi} - f'' \frac{\partial f}{\partial \xi}\right). \tag{19}$$

In (19) the primes now denote differentiation with respect to η. The parameter b is still defined by (15) except that now t is expressed in transformed variables and is given by

$$t = 1 - \left(1 - \frac{2\eta\sqrt{\xi}}{\sqrt{R_L}}\right)^{1/2}. \tag{20}$$

The boundary conditions for the continuity and momentum equations are:

$$y = 0, \quad u = 0, \quad v = 0 \text{ (no mass transfer)}; \; y = y_c, \; \partial u/\partial y = 0 \tag{21}$$

In terms of dimensionless quantities defined by (4) and in terms of a stream function expressed in physical coordinates with $y_c = L$; they become

$$\bar{y} = 0, \quad F = F' = 0, \quad \bar{y} = \sqrt{R_L}, \quad F'' = 0 \tag{22}$$

In terms of a stream function expressed in transformed coordinates, (22) become

$$\eta = 0, \quad f = f' = 0, \quad \eta_{sp} = \sqrt{R_L}/\xi, \quad f'' = 0 \tag{23a}$$

In our study we replace the outer boundary condition $f'' = 0$ by another boundary condition obtained by evaluating (19) at the boundary-layer edge (η_∞)

$$\frac{d}{d\xi}\frac{(f')^2}{2} = -\frac{dp^*}{d\xi} \tag{23b}$$

<u>Newton's Method</u>

The presence of $dp^*/d\xi$ term in either (14) or (19) introduces an additional unknown to the system given by (14) and (22) or by (19) and (23). Thus another equation is needed and we use conservation of mass. In the case of a channel, mass balance gives

$$u_0 L = \int_0^L u \, dy \tag{24}$$

In terms of dimensionless variables and stream function expressed in physical coordinates, (24) can be written as

$$1 = F(\bar{x}, \sqrt{R_L})/\sqrt{R_L} \tag{25}$$

When the stream function is expressed in transformed variables, we can put (24) in a form similar to (25), that is,

$$1 = f(\xi,\eta_{sp})/\eta_{sp} \tag{26}$$

Similarly for the case of a pipe, we can write equations similar to (25) and (26), respectively. They are

$$1 = 2F(\bar{x}, \sqrt{R_L})/\sqrt{R_L} \tag{27}$$

$$1 = 2f(\xi, \eta_{sp})/\eta_{sp} \tag{28}$$

Since $dp^*/d\xi$ is not known, it is obvious that an iteration procedure is necessary. In our study this is done by using Newton's method. We first solve the system given by (14) and (22) or by (19) and (23) for an assumed dp^*. This is a typical boundary-layer problem; for brevity we shall call it the standard problem. The next value of dp^* is obtained from Newton's method. For example, if we write (25) as

$$\phi(\beta^\nu) \equiv 1 - F(\bar{x}, \sqrt{R_L})/\sqrt{R_L} = 0, \quad (\partial\phi/\partial\beta)(\beta^\nu) \tag{29}$$

then the next value of $\beta^{\nu+1}$ is obtained from

$$\beta^{\nu+1} = \beta^\nu - \frac{\phi(\beta^\nu)}{(\partial\phi/\partial\beta)} \qquad \nu = 0, 1, 2, \ldots \tag{30}$$

Here we have denoted dp^* by $-\beta$ for convenience. The derivative of ϕ with respect to β is obtained from (29),

$$\frac{\partial\phi}{\partial\beta}(\beta^\nu) = -\frac{1}{\sqrt{R_L}}\frac{\partial F}{\partial\beta}(\bar{x}, \sqrt{R_L}) \tag{31}$$

The derivative of F with respect to β is obtained by solving a system of variational equations to be described later in the paper. The iteration process is repeated until

$$\left|\beta^{(\nu+1)}(\bar{x}_n) - \beta^\nu(\bar{x}_n)\right| < \alpha_1 \tag{32}$$

where α_1 is a small error tolerance.

Numerical Method for the Standard Problem

The solution of the equations of the standard problem (and the solution of the variational equations to be described in the next section) is obtained by using the two-point finite-difference method developed by H. B. Keller[1]. The application of the method to two-dimensional and three-dimensional boundary layers is described in some detail in refs. (2)-(4). Therefore, only a brief description of it for the system (19), (23) will be given here.

We introduce new dependent variables $u(\xi,\eta)$, $v(\xi,\eta)$ so that (19) can be written as the first-order system

$$f' = u \tag{33a}$$

$$u' = v \tag{33b}$$

$$(bv)' + \frac{1}{2} fv = \xi\frac{dp^*}{d\xi} + \xi\left(u\frac{\partial u}{\partial \xi} - v\frac{\partial f}{\partial \xi}\right) \tag{33c}$$

On net rectangles, shown in Fig. 1, we denote the net points by

$$\begin{aligned} &\xi_0 = 0, \qquad \xi_n = \xi_{n-1} + k_n, \qquad n = 1, 2, \ldots, N \\ &\eta_0 = 0, \qquad \eta_j = \eta_{j-1} + h_j, \qquad j = 1, 2, \ldots, J; \quad \eta_J = \eta_{sp} \end{aligned} \tag{34}$$

The quantities (f,u,v) at points (ξ_n, η_j) of the net are approximated by net functions denoted by (f_j^n, u_j^n, v_j^n). We also employ the notation for points and quantities midway between net points and for any net function g_j^n:

$$\begin{aligned} &\xi_{n-(1/2)} \equiv \frac{1}{2}(\xi_n + \xi_{n-1}), \qquad \eta_{j-(1/2)} \equiv \frac{1}{2}(\eta_j + \eta_{j-1}) \\ &g_j^{n-(1/2)} \equiv \frac{1}{2}(g_j^n + g_j^{n-1}) \qquad g_{j-(1/2)}^n \equiv \frac{1}{2}(g_j^n + g_{j-1}^n) \end{aligned} \tag{35}$$

The difference equations that are to approximate (33) are formulated by considering one mesh rectangle as in Fig. 1. We approximate (33a) and (33b) using centered difference quotients and average about the midpoint $(\xi_n, \eta_{j-(1/2)})$ of the segment P_2P_4 as follows:

$$h_j^{-1}(f_j^n - f_{j-1}^n) = u_{j-(1/2)}^n \tag{36a}$$

$$h_j^{-1}(u_j^n - u_{j-1}^n) = v_{j-(1/2)}^n \tag{36b}$$

Similarly, (33c) is approximated by centering about the midpoint $(\xi_{n-(1/2)}, \eta_{j-(1/2)})$ of the rectangle $P_1P_2P_3P_4$ to get

$$h_j^{-1}[(bv)_j^n - (bv)_{j-(1/2)}^n] - \alpha_n(u^2)_{j-(1/2)}^n + \left(\frac{1}{2} + \alpha_n\right)(fv)_{j-(1/2)}^n$$

$$+ \alpha_n[f_{j-(1/2)}^n v_{j-(1/2)}^{n-1} - v_{j-(1/2)}^n f_{j-(1/2)}^{n-1}] = T_{j-(1/2)}^{n-1} - \alpha_n\beta \tag{36c}$$

where

$$T_{j-(1/2)}^{n-1} = \alpha_n\left[(fv)_{j-(1/2)}^{n-1} - (u^2)_{j-(1/2)}^{n-1}\right] - h_j^{-1}\left[(bv)_j^{n-1} - (bv)_{j-1}^{n-1}\right] \tag{37a}$$

$$\alpha_n = \frac{\xi_{n-(1/2)}}{\xi_n - \xi_{n-1}}, \qquad \beta = (P^*)^{n-1} - (P^*)^n \tag{37b}$$

Equations (36) are imposed for $j = 1, 2, \ldots, J$. The wall boundary conditions in (23a) yield, at $\xi = \xi_n$

$$f_0^n = 0, \qquad u_0^n = 0 \tag{38a}$$

The outer boundary condition in (23b) yields, at $\xi = \xi_n$

$$(u^2)_J^n = (u^2)_J^{n-1} + 2\beta. \tag{38b}$$

If we assume $(f_j^{n-1}, u_j^{n-1}, v_j^{n-1})$ and β^n to be known for $0 \leq j \leq J$, then (36) for $1 \leq j \leq J$ and the boundary conditions (38) yield a nonlinear algebraic system of $3J + 3$ equations in as many unknowns (f_j^n, u_j^n, v_j^n). The system can be solved very effectively by using Newton's method. The important observation is that the linearized equations obtained by applying Newton's method to (36) and (38) form a block tridiagonal system (with 3×3 blocks), a system that can be solved in a very efficient manner as discussed in ref. 3.

Variational Equations

In order to calculate $\partial\phi/\partial\beta$ in (30) it is necessary to know $\partial f/\partial\beta$. For this reason we take the derivative of (36) with respect to β. This leads to the following linear difference equations, known as the variational equations for (36):

$$h_j^{-1}(G_j^n - G_{j-1}^n) = U_{j-(1/2)}^n \tag{39a}$$

$$h_j^{-1}(U_j^n - U_{j-1}^n) = V_{j-(1/2)}^n \tag{39b}$$

$$h_j^{-1}(b_j^n V_j^n - b_{j-1}^n V_{j-1}^n) - \alpha_n(u_j^n U_j^n + u_{j-1}^n U_{j-1}^n) + \frac{1}{2}\left(\frac{1}{2} + \alpha_n\right)(f_j^n V_j^n + v_j^n G_j^n + f_{j-1}^n V_{j-1}^n + v_{j-1}^n G_{j-1}^n)$$

$$+ \frac{1}{2}\alpha_n[v_{j-(1/2)}^{n-1}(G_j^n + G_{j-1}^n) - f_{j-(1/2)}^{n-1}(V_j^n + V_{j-1}^n)] = -\alpha_n. \tag{39c}$$

Similarly the boundary conditions yield

$$G_0^n = 0, \quad U_0^n = 0, \quad U_J^n = 1/u_J^n \tag{40}$$

Throughout (39) and (40) we have used the notation

$$G \equiv \partial f/\partial\beta, \qquad U \equiv \partial u/\partial\beta, \qquad V \equiv \partial v/\partial\beta \tag{41}$$

The system (39), (40) again forms a block tridiagonal system (with 3 x 3 blocks) that is solved by the previously mentioned factorization procedure. For details see refs. (1), (3), and (5).

Comparison with Experiment

We now show a comparison of calculated results with experiment for both laminar and turbulent flows in pipes. From the available literature on experimental data on pipe laminar flows, the best data comes from Pfenninger[6] who was able to maintain the laminar flow condition for a diameter-Reynolds number as high as 50,000. Our calculated results and the experimental results of Pfenninger are shown in Fig. 2. The experimental data were shown as continuous curves, not tabulated, which could account for some of the deviation near the beginning of the pipe.

Figure 3 shows a comparison of calculated and experimental pressure drop results for a laminar pipe flow as a function of $\bar{x}/4\sqrt{R_L}$. The experimental data are due to Shapiro, Siegel and Kline[7].

Figure 4 shows a comparison of calculated and experimental velocity profiles for a turbulent flow in the entrance region of a pipe. The experimental data are due to Barbin and Jones[8]. The calculations were made by using the eddy-viscosity formulation described in ref. 5. That formulation is not described here due to space limitations. As in laminar flows, again the agreement with experiment is satisfactory.

Acknowledgment

This work was supported by the National Science Foundation Grant No. GK-30981 and by the U.S. Army Research Office, Durham, under Contract DAHC 04-68-0006.

References

1. Keller, H.B., A New Difference Scheme for Parabolic Problems in "Numerical Solution of Partial Differential Equations," (S. Bramble, ed.), Vol. II, Academic Press, New York, 1970.

2. Keller, H.B. and Cebeci, T., Accurate Numerical Methods for Boundary-Layer Flow, I: Two-Dimensional Laminar Flows, in Lecture Notes in Physics, Proceedings of Second International Conference on Numerical Methods in Fluid Dynamics, Springer-Verlag, Berlin, 1971.

3. Keller, H.B. and Cebeci, T., Accurate Numerical Methods for Boundary-Layer Flow, II. Two-Dimensional Turbulent Flows, AIAA Journal, Vol. 10, No. 9, pp. 1193-1200, Sept. 1972.

4. Cebeci, T., Calculation of Three-Dimensional Boundary Layers, II: Three-Dimensional Flows in Cartesian Coordinates, to be published.

5. Cebeci, T. and Smith, A.M.O., Analysis of Turbulent Boundary Layers, to be published by Academic Press, Dec. 1974.

6. Pfenninger, W., Further Laminar Flow Experiments in a 40-Foot Long Two-Inch-Diameter Tube, Report No. AM-133, Northrop Aircraft, Hawthorne, Calif., Feb. 1951.

7. Shapiro, A.H., Siegel, R. and Kline, S.J., Friction Factor in the Laminar Entry Region of a Round Tube, Proceedings of the Second U.S. National Congress of Applied Mechanics, ASME, pp. 733-741, 1954.

8. Barbin, A.R. and Jones, J.B., Turbulent Flow in the Inlet Region of a Smooth Pipe, Journal of Basic Engineering, vol. 85, pp. 29-34, Mar. 1963.

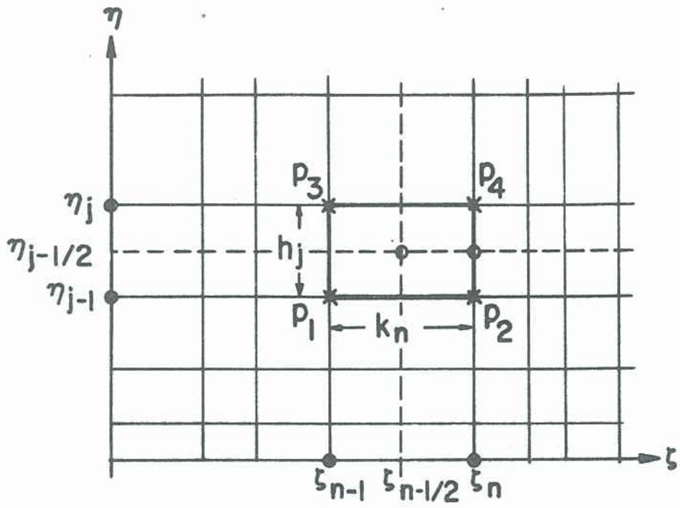

Fig. 1. Net rectangle for the difference equations.

Fig. 2. Comparison of calculated and experimental centerline velocity distribution in the entrance region of a pipe for laminar flow.

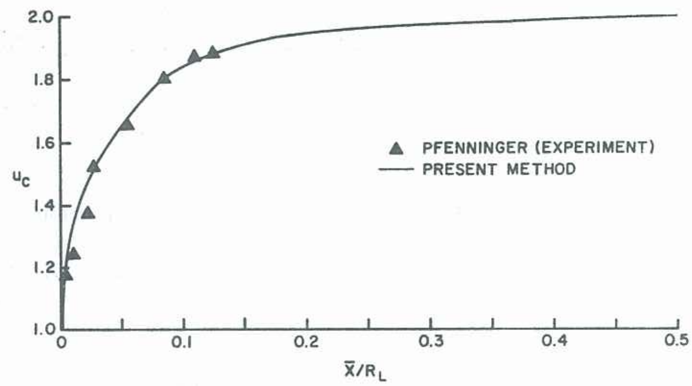

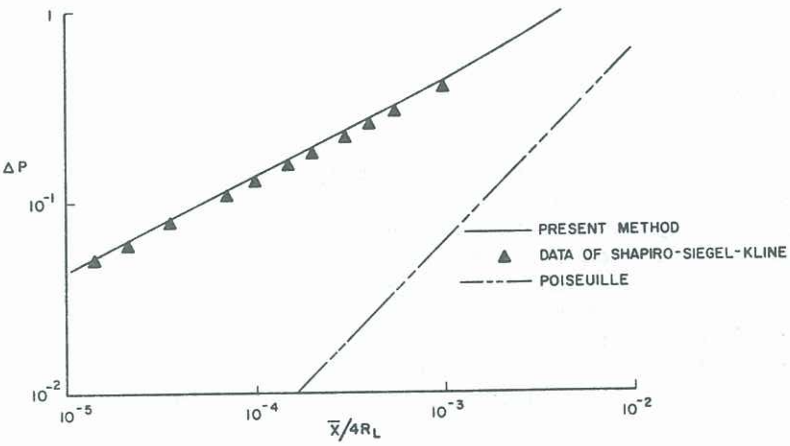

Fig. 3. Comparison of calculated and experimental pressure drop in the entrance region of a pipe for laminar flow.

Fig. 4. Comparison of calculated and experimental velocity profiles in the entrance region of a pipe for turbulent flow.